


## MATHEMATICS FOR SOCIAL AND ART SCIENCES

JEAN M.-S. LUBUMA  (Johannesburg)

ARSÈNE JAURES OUEMBA TASSÉ  (Johannesburg)

FRANCIS SIGNING  \* (Dschang)

BERGE TSANOU  (Dschang)

### Investigating the impact of isolation, self-isolation and environmental transmission on the spread of COVID-19: case study of Rwanda

**Abstract** In this work, we propose a ten-compartmental COVID-19 model with human to human and environment to human transmissions. A notational feature of this model is the consideration of the infected who escape from the self-isolation and later spread the disease. The model is rigorously analysed both theoretically and numerically. From the mathematical point of view, we prove that the disease-free equilibrium is globally asymptotically stable when the basic reproduction number  $\mathcal{R}_0^v$  is less than one, that is the disease dies out. When  $\mathcal{R}_0^v$  is greater than one, we prove that the model admits a unique endemic equilibrium, locally asymptotically stable, meaning that the disease would persist, at least inside the basin of attraction of the endemic equilibrium. The sensitivity analysis of the model highlights that the environmental transmission is the most influent parameter, which leads in an increasing number of infected individuals whenever it increases. The model is calibrated using the daily cumulative asymptomatic cases in Rwanda reported from the 1 April 2022 to the 14 June 2022. We found that the basic reproduction number is equal to 0.6479 and most infected people in Rwanda during this period of time are asymptomatic. We investigate the impact of isolation and self-isolation to reduce the disease burden, and both sensitivity analysis and numerical analysis show that the isolation has more effect on the dynamics of the infected than the self-isolation. We also prove that, the individuals who escape from the self-isolation, contribute, but weakly to the increasing of the number of infected individuals.

*2010 2020 Mathematics Subject Classification:* Primary: 62J05; Secondary: 92D20.

*Key words and phrases:* COVID-19; Isolation; Self-isolation; Environmental transmission; Escaper; Global stability; Sensitivity analysis.

**1. Introduction** The Coronavirus disease 2019 (COVID-19) started in China in December 2019 and was rapidly spread around that country and all over the world. It was declared a Public Health Emergency of International Concern by the World Health Organization (WHO) on January 30 2020.

---

\* The corresponding author

As of June 30 2023, the disease have caused about 767,726,861 confirmed cases, among them 6,948,764 succumbed to it [4]. According to the WHO, the COVID-19 is transmitted through respiratory droplets and contact routes [5]. Droplets transmission occurs when a person is in close contact (within one meter) with someone who has respiratory symptoms (e.g. coughing or sneezing). The transmission may also occur through fomites in the immediate environment around the infected persons.

The management of COVID-19 patients involves treatment and preventive measures such as the isolation, the disinfection of the environment, the wearing of protective masks and other basic measures like the physical distancing, the covering of coughs and sneezes with a tissue or inner elbow and regularly hand washing with soap or alcohol gel. It is well known that more than 80% of COVID-19 cases are asymptomatic infected or present just mild symptoms of the disease [26]. Thus, so that medical center are not overwhelmed, countries with a great number of cases (France, Ukraine, Switzerland, Italy, etc) implemented the self-isolation measure of infected showing benign symptoms [9]. The self-isolation means staying at home and taking common sense precautions and eventually treatment to avoid close contact with those you live with and visitors [9]. The isolation centres are only required for critical cases, that is for the infected requiring intensive care management and ventilators. Despite these plethora of measures, to contain the COVID-19 pandemic, the disease still persists in many countries. Thus, one should question the significance of these control strategies to mitigate the ongoing pandemic. It is well known that mathematical and simulation are important tools that can be used to control human diseases and to assess the relevance of implemented control strategies [6, 10].

To predict, understand and evaluate the relevance of control strategies implemented against COVID-19, several mathematical models have been addressed, with some investigating the impact of the environmental transmission. In [20] for instance, the authors investigated the impact of contact tracing and quarantine in the evolution of the COVID-19 pandemic. Their model is applied to the early stage of the COVID-19 outbreak in Poland. They showed that the implementation of contact tracing may have prevented from 50% to over 90% of cases. Moreover, from their view, the effects of quarantine are limited by the fraction of undiagnosed cases. The paper [18] formulated a mathematical model for the dynamical transmission of COVID-19 in the context of sub-saharan Africa, including the environmental transmission. They afterwards calibrated their model to the weekly data in Cameroon and Gabon, during and after the lockdown. During the estimation period, their findings showed that  $\mathcal{R}_0 = 1.8377$  in Cameroon and  $\mathcal{R}_0 = 1.0379$  in Gabon. Moreover, they proved that the number of undetected cases are high in Cameroon and Gabon and that the lockdown was not the solution to the outbreak in Cameroon, but was the solution to it in Gabon. A comparative

study that they have done during the estimation period shows that the environmental transmission of COVID-19 is greater than the human to human transmission in Cameroon ( $\mathcal{R}_{0h} = 0.05721$  and  $\mathcal{R}_{0v} = 1.78051$ , with  $\mathcal{R}_{0h}$  and  $\mathcal{R}_{0v}$  the contribution of human–human transmission and environment–human transmission to the basic reproduction number). But they obtained an opposite result in Gabon ( $\mathcal{R}_{0h} = 0.63899$  and  $\mathcal{R}_{0v} = 0.39894$ ). In the work presented in [7], the authors used a compartmental model to analyse the transmission dynamics of COVID-19 in South Africa and to assess the impact of various control strategies (distancing measure, self-isolation, isolation, lockdown). They numerically showed that if the lockdown measures in South Africa were implemented a week later than the 26 March, 2020 date it was implemented, it would have led an extension of the predicted peak time of the pandemic, and causing about 10% more cumulative deaths. Moreover they highlighted the effectiveness of self-isolation and contact tracing in curtailing the pandemic in South Africa. Furthermore, they proved that the environmental contamination has a substantial contribution of 19% to the control reproduction number. However, to the best of our knowledge, no research project on COVID-19 investigates the impact of the infected who refuse to comply to the self-isolation measure. The purpose of this project is to fill this weakness. To do so, we proposed in this work a compartmental model which considers: (a) human to human transmission as well as the environmental transmission; (b) the isolation and the self-isolation measures to mitigate the transmission of the disease. We assume the infected settled in isolation are effectively isolated in the sense that they are not in contact with the whole population and are therefore not infectious; (c) Some self-isolated infected may escape (refuse to comply) the self-isolation measure and infect susceptible individuals. The propounded model is rigorously analysed. From the mathematical point of view, we prove the positivity of the model variables, compute the basic reproduction number and study the stability of equilibria. The sensitivity analysis of the model is done, in order to determine the parameters which are influential on the dynamics of the infection. Numerically, our model is calibrated using the daily cumulative asymptomatic cases in Rwanda reported from the 1 April 2022 to the 14 June 2022. Moreover, we investigate the usefulness of the isolation, self-isolation, the influence of the environmental transmission and explore the impact of the transmission of the individuals who refuse to comply to the self-isolation measure.

The rest of the paper is organized as follows. In Section 2, the model is formulated in a comprehensive manner. Section 3 presents the well-posedness of the model and explores the stability of its equilibria. The sensitivity analysis is developed in Section 4. The model validation and the numerical analysis are provided in Section 5. Finally, the conclusion of the work is presented in Section 6.

## 2. Model formulation

**2.1. Main assumptions** In order to simplify the model and for a better understanding, we assume the hypothesis.

- The massive tests screening is not considered in the model formulation. Thus, the individuals in latent period as well as the asymptomatic COVID-19 infected are not sent in self-isolation. Indeed, the latently infected individuals and the asymptomatic cases seem healthy like the susceptible individuals, and almost all of them ignore their epidemiological status, since they are undiagnosed.
- The symptomatic COVID-19 infected may only recover after being diagnosed. In fact after a positive COVID-19 diagnosis test, the infected undergo proper treatment, whether they are isolated or even self-isolated.

**2.2. Model variables and equations derivations** The total population of humans at time  $t$ ,  $N(t)$  is composed of ten disjoint epidemiological classes: the individuals susceptible to the COVID-19 infection,  $S(t)$ ; the individuals exposed to the COVID-19 infection,  $E(t)$ ; the carrier COVID-19 individuals,  $C(t)$  (this class refer to the asymptomatic infected individuals); the infected individuals who exhibit moderate/mild symptoms of COVID-19,  $I_m(t)$ ; the infected individuals with severe symptoms,  $I_s(t)$ ; the self-isolated individuals,  $Q(t)$ ; the hospitalized or isolated individuals,  $H(t)$ ; the individuals who escape from the self-isolation,  $L(t)$ ; and the recovered individuals,  $R(t)$ . Since only few individuals have contracted the COVID-19 twice [12], the recovered will be assumed immune. Therefore, at time  $t$ ,  $N(t)$  is given by:

$$N(t) = S(t) + E(t) + C(t) + I_m(t) + I_s(t) + Q(t) + L(t) + H(t) + R(t). \quad (1)$$

Apart from the human variables, we introduce a compartment  $V(t)$ , which is the concentration of the SARS-CoV-2 virus in the environment at time  $t$ . The account of this compartment is motivated by the fact that COVID-19 infected cases shed SARS-CoV-2 virus in the environment when they sneeze, talk or cough and the people who touch objects and surfaces on which these droplets have landed, and then touch their eyes, noses or mouths, can be infected [7].

Let  $\mu$  be the natural mortality rate and  $\Lambda$  the recruitment rate of the susceptible individuals. The susceptible population can be infected through human to human contacts with the individuals in the compartments  $C$ ,  $I_m$ ,  $I_s$  and  $L$  at the rates  $\beta_h, \varepsilon_1\beta_h, \varepsilon_2\beta_h, \varepsilon_3\beta_h$ , respectively (where  $\varepsilon_i, i = 1, 2, 3$  are the modification parameters) or after contact with a polluted environment, at the rate  $\beta_v$ . Once infected, they enter in a latent period. At the end of latency, they may either: (i) exhibit severe symptoms, at the rate  $p\gamma$ , (ii) moderate symptoms, at the rate  $q(1-p)\gamma$ , or simply be (iii) the carrier infected individuals, at the rate  $(1-q)(1-p)\gamma$ . We assume that the individuals asymptomatic may progress to moderate symptoms, and this at the rate  $\phi_1$

or recover at the rate  $\kappa_1$ . While those with moderate symptoms may progress to severe symptoms at the rate  $\phi_2$  or are self-isolated at the rate  $\alpha$  (after being diagnosed). Self-isolated individuals may escape from the isolation at the rate  $f\eta$ , recover at the rate  $\tau(1-f)\eta$  (since they received drugs or natural products after a positive diagnosis) or may progress to severe symptoms, at the rate  $(1-\tau)(1-f)\eta$  before their admission in isolation settings. Indeed, the infected who exhibit severe symptoms are isolated inside hospital, at the rate  $\theta$ . But in this compartment, they can decrease due to COVID-19 at the rate  $\chi$ . Those who escape from the self-isolation would continue their treatment and may recover at the rate  $\kappa_2$  or progress towards severe symptoms, at the rate  $\delta$ .

The infected who are outside isolation, that is those in the compartments  $C, I_m, I_s$  and  $L$  shed the Coronavirus in the environment at the rates,  $\psi_1, \psi_2, \psi_3$  and  $\psi_4$ , respectively. We call  $\mu_v$  the decay rate of the Coronavirus in the environment.

From above, the human to human force of infection is modelled by

$$\lambda_h(t) = \frac{\beta_h(C(t) + \varepsilon_1 I_m(t) + \varepsilon_2 I_s(t) + \varepsilon_3 L(t))}{N(t) - Q(t) - H(t)} \tag{2}$$

and the force of infection due to environmental transmission is represented by:

$$\lambda_v(t) = \beta_v V(t). \tag{3}$$

Hence the COVID-19 force of infection  $\lambda$  is:

$$\lambda(t) := \lambda_h(t) + \lambda_v(t) = \frac{\beta_h(C(t) + \varepsilon_1 I_m(t) + \varepsilon_2 I_s(t) + \varepsilon_3 L(t))}{N(t) - Q(t) - H(t)} + \beta_v V(t). \tag{4}$$

A schematic model flowchart is depicted in Figure 1.

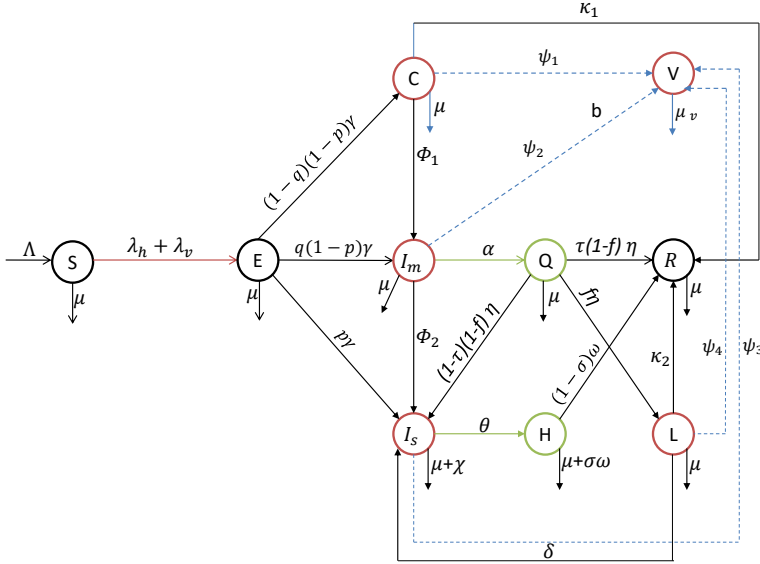


Figure 1: Diagram showing the interactions between the compartments.

The corresponding system of differential equations is:

$$\left\{ \begin{array}{l} \frac{dS}{dt} = \Lambda - \frac{\beta_h(C + \varepsilon_1 I_m + \varepsilon_2 I_s + \varepsilon_3 L)S}{N - Q - H} - \beta_v V S - \mu S, \\ \frac{dE}{dt} = \frac{\beta_h(C + \varepsilon_1 I_m + \varepsilon_2 I_s + \varepsilon_3 L)S}{N - Q - H} + \beta_v V S - (\mu + \gamma)E, \\ \frac{dQ}{dt} = \alpha I_m - (\mu + \eta)Q, \\ \frac{dC}{dt} = (1 - q)(1 - p)\gamma E - (\mu + \phi_1 + \kappa_1)C, \\ \frac{dI_m}{dt} = q(1 - p)\gamma E + \phi_1 C - (\mu + \phi_2 + \alpha)I_m, \\ \frac{dI_s}{dt} = (1 - \tau)(1 - f)\eta Q + p\gamma E + \phi_2 I_m + \delta L - (\mu + \theta + \chi)I_s, \\ \frac{dH}{dt} = \theta I_s - (\mu + \omega)H, \\ \frac{dL}{dt} = f\eta Q - (\mu + \delta + \kappa_2)L, \\ \frac{dR}{dt} = \tau(1 - f)\eta Q + (1 - \sigma)\omega H + \kappa_1 C + \kappa_2 L - \mu R, \\ \frac{dV}{dt} = \psi_1 C + \psi_2 I_m + \psi_3 I_s + \psi_4 L - \mu_v V. \end{array} \right. \quad (5)$$

All the parameters of Model (5) and their definitions are gathered in Table 1 below. For biological reasons, all the parameters are assumed nonnegative.

Table 1: Description of the parameters for the formulation of the model.

Symbol	Description
$\Lambda$	Recruitment rate of susceptible individuals.
$\mu$	Natural dead rate.
$\psi_1$	Shedding rate of COVID-19 in the environment by the carrier individuals.
$\psi_2$	Shedding rate of COVID-19 in the environment by the infected with moderate symptoms.
$\chi$	Death rate due to severe COVID-symptoms.
$\psi_3$	Shedding rate of COVID-19 in the environment by the infected individuals with moderate symptoms.
$\psi_4$	Shedding rate of COVID-19 in the environment by the individuals who escape from the self isolation.
$\gamma$	Incubation period rate of infected individuals.
$\beta_h$	Effective transmission of asymptomatic infected individuals.
$\beta_v$	Effective transmission of COVID-19, due to contact with the environment.
$\mu_v$	Decay rate of COVID-19 in the environment
$p$	Proportion of formerly exposed individuals who become infected with severe symptoms.
$q$	Proportion of formerly exposed individuals who become infected with moderate symptoms.
$\alpha$	Rate of infected individuals with moderate symptoms who enter in self-isolation.
$\phi_2$	Transfer rate from the compartment $I_m$ to the compartment $I_s$ .
$\phi_1$	Rate of asymptomatic individuals who develop moderate symptoms.
$\theta$	Hospitalization rate of individuals with severe symptoms.
$\delta$	Transfer rate from the compartment $L$ to the compartment $I_s$ .
$\omega$	Proportion of individuals who leave hospital due to illness-induced death or healing.
$\sigma\omega$	Proportion of individuals who leave hospital due to illness-induced death.
$\eta$	Proportion of individuals leaving quarantine by any other means than natural death.
$f\eta$	Proportion of individuals who escape from the isolation.
$\tau(1 - f)\eta$	Proportion of individuals leaving the self-isolation by the recovering.
$\kappa_1$	Recovery rate of the asymptomatic individuals.
$\kappa_2$	Recovery rate of escapers from the self-isolation.
$\{\varepsilon_i\}_{1 < i < 3}$	Infectivity modification parameters

### 3. Mathematical analysis

**3.1. Well-posedness of the model** In this subsection, we prove that Model (5) is well-posed in the epidemiological point of view, that is the solutions of the model exist for all time, they remain positive and belong to a compact set. This result, which the proof is postponed to Appendix A is summarized in the following theorem.

THEOREM 3.1 Assume

$$S(0) > 0, E(0), Q(0), C(0), I_m(0), I_s(0), H(0), L(0), R(0), V(0) \geq 0.$$

Then for every  $t > 0$ ,

$$S(t) > 0, E(t), Q(t), C(t), I_m(t), I_s(t), H(t), L(t), R(t), V(t) \geq 0.$$

Furthermore, the set

$$\Omega = \left\{ (S, E, Q, C, I_m, I_s, H, L, R, V) \in \mathbb{R}_+^{10}, N(t) \leq \frac{\Lambda}{\mu}, \right. \\ \left. V(t) \leq \frac{\Lambda(\psi_1 + \psi_2 + \psi_3 + \psi_4)}{\mu_v \mu} \right\}.$$

is positively invariant.

Thanks to Theorem 3.1, our model admits a unique global solution for non-negative initial conditions.

### 3.2. The basic reproduction number for System (5)

For notational elegance and simplicity, we define the following parameters.

$$\begin{aligned} d_1 &= (\mu + \gamma), d_2 = (\mu + \eta), d_3 = (\mu + \phi_1 + \kappa_1), b_3 = p\gamma, \\ d_4 &= (\mu + \phi_2 + \alpha), d_6 = (\mu + \omega), d_7 = (\mu + \delta + \kappa_2), \\ b_1 &= (1 - q)(1 - p)\gamma, b_2 = q(1 - p)\gamma, d_5 = (\mu + \theta + \chi), \\ b_4 &= (1 - \tau)(1 - f)\eta, b_6 = \tau(1 - f)\eta, b_7 = (1 - \sigma)\omega, \\ d_8 &= d_1 d_2 d_3 d_4 d_5 d_7, d_9 = d_3 d_4 d_2 d_7 d_5 d_6, b_5 = f\eta, \\ K_1 &= \alpha (b_2 d_3 + \phi_1 b_1), K_2 = b_2 d_3 + \phi_1 b_1, \\ K_8 &= b_4 d_7 + \delta b_5, K_{10} = d_7 \phi_2 d_2 + d_7 b_4 \alpha + \delta b_5 \alpha, \\ K_9 &= \phi_1 (d_7 \phi_2 d_2 + d_7 b_4 \alpha + \delta b_5 \alpha) K_{11} = \theta (b_4 d_7 + \delta b_5), \\ K_{12} &= \theta \phi_1 (d_7 \phi_2 d_2 + d_7 b_4 \alpha + \delta b_5 \alpha), \\ K_{13} &= \theta (d_7 \phi_2 d_2 + d_7 b_4 \alpha + \delta b_5 \alpha), \\ K_{17} &= \kappa_2 d_6 d_5, + b_7 \theta \delta, K_{21} = \psi_4 d_5 + \psi_3 \delta, \\ K_{18} &= \psi_3 b_4 d_7 + b_5 \psi_4 d_5 + b_5 \psi_3 \delta, K_5 = b_5 \alpha (b_2 d_3 + \phi_1 b_1), \\ K_{14} &= b_6 d_6 d_5 d_7 + b_7 \theta b_4 d_7 + b_5 \kappa_2 d_6 d_5 + b_5 b_7 \theta \delta, \\ K_{15} &= \kappa_1 d_6 d_5 d_7 d_2 d_4 + b_6 \alpha \phi_1 d_6 d_5 d_7 + b_7 \theta \phi_1 d_7 \phi_2 d_2 \\ &\quad + b_7 \theta \phi_1 d_7 b_4 \alpha + b_5 \alpha \phi_1 \kappa_2 d_6 d_5 + b_5 \alpha \phi_1 b_7 \theta \delta, \\ K_{16} &= b_6 \alpha d_6 d_5 d_7 + b_7 \theta d_7 \phi_2 d_2 + b_7 \theta d_7 b_4 \alpha \\ &\quad + b_5 \alpha \kappa_2 d_6 d_5 + b_5 \alpha b_7 \theta \delta, \\ K_{19} &= \psi_1 d_5 d_7 d_2 d_4 + \psi_2 \phi_1 d_5 d_7 d_2 + \psi_3 \phi_1 d_7 \phi_2 d_2 \\ &\quad + \psi_3 \phi_1 d_7 b_4 \alpha + b_5 \alpha \phi \psi_4 d_5 + b_5 \alpha \phi_1 \psi_3 \delta, \\ K_{20} &= \psi_2 d_5 d_7 d_2 + \psi_3 d_7 \phi_2 d_2 + \psi_3 d_7 b_4 \alpha + b_5 \alpha \psi_4 d_5 + b_5 \alpha \psi_3 \delta, \\ K_3 &= d_7 b_3 d_2 d_4 d_3 + d_7 \phi_2 d_2 b_2 d_3 + d_7 \phi_2 d_2 \phi_1 b_1 + d_7 b_4 \alpha b_2 d_3 \\ &\quad + d_7 b_4 \alpha \phi_1 b_1 + \delta b_5 \alpha b_2 d_3 + \delta b_5 \alpha \phi_1 b_1, \\ K_4 &= \theta (d_7 b_3 d_2 d_4 d_3 + d_7 \phi_2 d_2 b_2 d_3 + d_7 \phi_2 d_2 \phi_1 b_1 + d_7 b_4 \alpha b_2 d_3 \\ &\quad + d_7 b_4 \alpha \phi_1 b_1 + \delta b_5 \alpha b_2 d_3 + \delta b_5 \alpha \phi_1 b_1), \end{aligned} \tag{6}$$





and

$$W = \begin{pmatrix} d_1 & 0 & 0 & 0 & 0 & 0 & 0 & 0 & 0 \\ 0 & d_2 & 0 & -\alpha & 0 & 0 & 0 & 0 & 0 \\ -b_1 & 0 & d_3 & 0 & 0 & 0 & 0 & 0 & 0 \\ -b_2 & 0 & -\phi_1 & d_4 & 0 & 0 & 0 & 0 & 0 \\ -b_3 & -b_4 & 0 & -\phi_2 & d_5 & 0 & -\delta & 0 & 0 \\ 0 & 0 & 0 & 0 & -\theta & d_6 & 0 & 0 & 0 \\ 0 & -b_5 & 0 & 0 & 0 & 0 & d_7 & 0 & 0 \\ 0 & -b_6 & -\kappa_1 & 0 & 0 & -b_7 & -\kappa_2 & \mu & 0 \\ 0 & 0 & -\psi_1 & -\psi_2 & -\psi_3 & 0 & -\psi_4 & 0 & \mu_v \end{pmatrix}.$$

The inverse of the matrix  $W$  is:

$$W^{-1} = \begin{pmatrix} d_1^{-1} & 0 & 0 & 0 & 0 & 0 & 0 & 0 & 0 \\ \frac{K_1}{d_3 d_1 d_4 d_2} & d_2^{-1} & \frac{\alpha \phi_1}{d_3 d_4 d_2} & \frac{\alpha}{d_4 d_2} & 0 & 0 & 0 & 0 & 0 \\ \frac{B_1}{d_3 d_1} & 0 & d_3^{-1} & 0 & 0 & 0 & 0 & 0 & 0 \\ \frac{K_2}{d_3 d_1 d_4} & 0 & \frac{\phi_1}{d_3 d_4} & d_4^{-1} & 0 & 0 & 0 & 0 & 0 \\ \frac{K_3}{d_8} & \frac{K_8}{d_5 d_7 d_2} & \frac{K_9}{d_5 d_7 d_2 d_4 d_3} & \frac{K_{10}}{d_5 d_7 d_2 d_4} & d_5^{-1} & 0 & \frac{\delta}{d_5 d_7} & 0 & 0 \\ \frac{K_4}{d_6 d_8} & \frac{K_{11}}{d_6 d_5 d_7 d_2} & \frac{K_{12}}{d_6 d_5 d_7 d_2 d_4 d_3} & \frac{K_{13}}{d_6 d_5 d_7 d_2 d_4} & \frac{\theta}{d_6 d_5} & d_6^{-1} & \frac{\theta \delta}{d_6 d_5 d_7} & 0 & 0 \\ \frac{K_5}{d_3 d_1 d_4 d_2 d_7} & \frac{b_5}{d_2 d_7} & \frac{b_5 \alpha \phi_1}{d_3 d_4 d_2 d_7} & \frac{b_5 \alpha}{d_4 d_2 d_7} & 0 & 0 & d_7^{-1} & 0 & 0 \\ \frac{K_6}{d_6 d_8 \mu} & \frac{K_{14}}{d_6 d_5 d_7 d_2 \mu} & \frac{K_{15}}{d_6 d_5 d_7 d_2 d_4 d_3 \mu} & \frac{K_{16}}{d_6 d_5 d_7 d_2 d_4 \mu} & \frac{b_7 \theta}{d_6 d_5 \mu} & \frac{b_7}{d_6 \mu} & \frac{K_{17}}{d_6 d_5 d_7 \mu} & \mu^{-1} & 0 \\ \frac{K_7}{d_8 \mu_v} & \frac{K_{18}}{d_5 d_7 d_2 \mu_v} & \frac{K_{19}}{d_5 d_7 d_2 d_4 d_3 \mu_v} & \frac{K_{20}}{d_5 d_7 d_2 d_4 \mu_v} & \frac{\psi_3}{d_5 \mu_v} & 0 & \frac{K_{21}}{d_5 d_7 \mu_v} & 0 & \mu_v^{-1} \end{pmatrix},$$

The next generation matrix, defined by  $FW^{-1}$  is given as:

$$FW^{-1} = \begin{pmatrix} \mathcal{R}_0^h + \mathcal{R}_0^v & \star & \star & \star & \star & \star & \star & 0 & \star \\ 0 & 0 & 0 & 0 & 0 & 0 & 0 & 0 & 0 \\ 0 & 0 & 0 & 0 & 0 & 0 & 0 & 0 & 0 \\ 0 & 0 & 0 & 0 & 0 & 0 & 0 & 0 & 0 \\ 0 & 0 & 0 & 0 & 0 & 0 & 0 & 0 & 0 \\ 0 & 0 & 0 & 0 & 0 & 0 & 0 & 0 & 0 \\ 0 & 0 & 0 & 0 & 0 & 0 & 0 & 0 & 0 \\ 0 & 0 & 0 & 0 & 0 & 0 & 0 & 0 & 0 \\ 0 & 0 & 0 & 0 & 0 & 0 & 0 & 0 & 0 \end{pmatrix},$$

where the  $\star$  account for terms which are not useful in the sequel,

$$\mathcal{R}_0^h = \frac{\beta_h b_1}{d_3 d_1} + \frac{\beta_h \varepsilon_1 K_2}{d_3 d_1 d_4} + \frac{\beta_h \varepsilon_2 K_3}{d_8} + \frac{\beta_h \varepsilon_3 K_5}{d_3 d_1 d_4 d_2 d_7}$$

and

$$\mathcal{R}_0^v = \frac{\beta_v \Lambda K_7}{d_8 \mu \mu_v}.$$

Thus, the basic reproduction number  $\mathcal{R}_0^{av}$ , which is the spectral radius of the matrix  $FW^{-1}$  is given by:

$$\mathcal{R}_0^{av} = \mathcal{R}_0^h + \mathcal{R}_0^v$$

REMARK 3.1 In the absence of environmental contamination, that is when  $\beta_v = 0$ , the basic reproduction number of Model (5) simplifies to  $\mathcal{R}_0^h$ . Clearly,  $\mathcal{R}_0^{av} > \mathcal{R}_0^h$ .

The environmental transmission increases the disease level. Moreover, by simple computations, one gets

$$\left\{ \begin{aligned} \frac{\partial \mathcal{R}_0^{av}}{\partial \beta_v} &= \frac{\Lambda K_7}{d_8 \mu \mu_v}, & \frac{\partial \mathcal{R}_0^{av}}{\partial \psi_4} &= \frac{\beta_v \Lambda (b_5 \alpha d_5 b_2 d_3 + b_5 \alpha d_5 \phi_1 b_1)}{d_8 \mu \mu_v}, \\ \frac{\partial \mathcal{R}_0^{av}}{\partial \psi_1} &= \frac{\beta_v \Lambda b_1 d_5 d_7 d_2 d_4}{d_8 \mu \mu_v}, \\ \frac{\partial \mathcal{R}_0^{av}}{\partial \psi_2} &= \frac{\beta_v \Lambda (d_5 d_7 d_2 b_2 d_3 + d_5 d_7 d_2 \phi_1 b_1)}{d_8 \mu \mu_v}, \\ \frac{\partial \mathcal{R}_0^{av}}{\partial \psi_3} &= \frac{\beta_v \Lambda (d_7 b_3 d_2 d_4 d_3 + d_7 \phi_2 d_2 b_2 d_3)}{d_8 \mu \mu_v} \\ &\quad + \frac{\beta_v \Lambda (d_7 \phi_2 d_2 \phi_1 b_1 + d_7 b_4 \alpha b_2 d_3)}{d_8 \mu \mu_v} \\ &\quad + \frac{\beta_v \Lambda (d_7 b_4 \alpha \phi_1 b_1 + b_5 \alpha \delta b_2 d_3 + b_5 \alpha \delta \phi_1 b_1)}{d_8 \mu \mu_v}. \end{aligned} \right. \tag{8}$$

All these derivatives are positive. Thus, the basic reproduction number  $\mathcal{R}_0^{av}$  is an increasing function of the shedding rates of Coronavirus and an increasing function of the transmission due to the environment.

The relevance of the basic reproduction number  $\mathcal{R}_0^{av}$  is established in the following result [25].

LEMMA 3.2 The DFE  $Q_0$  of System (5) is locally asymptotically stable (LAS) if  $\mathcal{R}_0^{av} < 1$  and it is unstable whenever  $\mathcal{R}_0^{av} > 1$ .

The epidemiological implication of Lemma 3.2 is that the COVID-19 can be eliminated from the community when  $\mathcal{R}_0^{av} < 1$  and if the initial sizes of the different subpopulations of the model are in the basin of attraction of the DFE  $Q_0$ . For a better control of the disease, the GAS of the DFE is needed. This will be done further. In the following paragraph, we will discuss the existence of positive equilibria for Model (5).

**3.3. Existence of the endemic equilibrium for Model (5)** Let  $\mathcal{E}^* = (S^*, E^*, Q^*, C^*, I_m^*, I_s^*, H^*, L^*, R^*, V^*)$  be any positive endemic equilibrium of

System (5) and  $\lambda^*$  be the force of infection at the equilibrium. The components of the endemic equilibrium  $\mathcal{E}^*$  takes the form:

$$\left\{ \begin{array}{l} S^* = \frac{\Lambda}{\mu + \lambda^*}, E^* = \frac{\Lambda \lambda^*}{(\mu + \lambda^*) d_1}, Q^* = \frac{\lambda^* \Lambda K_1 d_7 d_5}{(\mu + \lambda^*) d_8}, \\ C^* = \frac{\lambda^* \Lambda b_1 d_4 d_2 d_7 d_5}{(\mu + \lambda^*) d_8}, I_m^* = \frac{\lambda^* \Lambda K_2 d_2 d_7 d_5}{(\mu + \lambda^*) d_8}, \\ I_s^* = \frac{\lambda^* \Lambda K_3}{(\mu + \lambda^*) d_8}, H^* = \frac{\Lambda \lambda^* K_4}{(\mu + \lambda^*) d_8 d_6}, \\ L^* = \frac{\Lambda \lambda^* K_5 d_5 d_6}{(\mu + \lambda^*) d_8 d_6}, R^* = \frac{\lambda^* \Lambda K_6}{(\mu + \lambda^*) d_8 d_6 \mu}, \\ V^* = \frac{\lambda^* \Lambda K_7 d_6}{(\mu + \lambda^*) d_8 d_6 \mu_v}, \end{array} \right. \quad (9)$$

where  $\lambda^*$  is the value of the infection force at  $\mathcal{E}^*$ .

Substituting the expressions in (9) into the force of infection at  $\mathcal{E}^*$  shows that the non-zero equilibrium of Model (5) satisfies the following quadratic equation in  $\lambda^*$ :

$$a (\lambda^*)^2 + b \lambda^* - c (\mathcal{R}_0^{av} - 1) = 0, \quad (10)$$

where  $a$ ,  $b$  and  $c$  are as follows:

$$\begin{aligned} a &= (d_9 \mu + b_1 d_4 d_2 d_7 d_5 d_6 \mu + K_2 d_2 d_7 d_5 d_6 \mu + K_3 d_6 \mu + K_5 d_5 d_6 \mu + K_6) \Lambda \mu_v, \\ b &= \Lambda d_8 d_6 \mu \mu_v (1 - \mathcal{R}_0^h) + \Lambda \mu \mu_v (1 - \mathcal{R}_0^v) \\ &\quad \cdot (d_9 \mu + b_1 d_4 d_2 d_7 d_5 d_6 \mu + K_2 d_2 d_7 d_5 d_6 \mu + K_3 d_6 \mu + K_5 d_5 d_6 \mu + K_6), \\ c &= \Lambda \mu^2 d_8 d_6 \mu_v. \end{aligned}$$

Note that  $a > 0$  and  $b > 0$  whenever  $\mathcal{R}_0^{av} \leq 1$ . Furthermore,  $c > 0$  whenever  $\mathcal{R}_0^{av} > 1$ . Hence, one has the result.

**THEOREM 3.3** For System (5), the following statements hold.

- (i) If  $\mathcal{R}_0^{av} > 1$  then System (5) admits a unique endemic equilibrium.
- (ii) If  $\mathcal{R}_0^{av} \leq 1$ , Model (5) do not admits a positive equilibrium, the disease-free equilibrium is its unique steady state.

**COROLLARY 3.4** When  $\mathcal{R}_0^{av} > 1$ , the components of the endemic equilibrium for Model (5) are given by Eqs. (9), with

$$\lambda^* = \frac{-b + \sqrt{b^2 + 4ac}}{2a}. \quad (11)$$

The components of  $\mathcal{E}^*$  are obtained by substituting this positive root of (10) into the steady-state components in (9).

The paragraph below deals with the global asymptotic stability of the DFE when  $\mathcal{R}_0^{av} \leq 1$

### 3.4. Global asymptotic stability of the DFE

**THEOREM 3.5** The DFE point  $Q_0$  of Model (5) in  $\Omega$  is GAS if  $\mathcal{R}_0^{av} < 1$ .

Let  $x = (E, Q, C, I_m, I_s, H, L, R, V)^T$  and  $y = (S, R)^T$ , be the parts of infected and uninfected states for Model (5), respectively. System (5) can be rewritten as

$$\begin{cases} \frac{dx}{dt} = (F - W)x - f(x, y) \\ \frac{dy}{dt} = g(x, y), \end{cases} \tag{12}$$

where  $F$  and  $W$  are given as,

$$\begin{aligned} f(x, y) &= \left( \frac{(E + C + I_m + I_s + L + R)\beta_h(C + \varepsilon_1 I_m + \varepsilon_2 I_s + \varepsilon_3 L)}{S + E + C + I_m + I_s + L + R} \right. \\ &\quad \left. + \beta_v V \left( \frac{\Lambda}{\mu} - S \right), 0, 0, 0, 0, 0, 0, 0 \right)^T, \\ g(x, y) &= \left( \Lambda - \frac{\beta_h(C + \varepsilon_1 I_m + \varepsilon_2 I_s + \varepsilon_3 L)S}{S + E + C + I_m + I_s + L + R} - \beta_v V S - \mu S, 0 \right)^T \end{aligned}$$

Since we are in  $\Omega$ , it is clear that  $S \leq \Lambda/\mu$ . Thus,  $f(x, y) \geq 0$  in  $\Omega$ . Therefore,  $dx/dt \leq (F - W)x$ . Consider now the following auxiliary linear system

$$\frac{d\tilde{x}}{dt} = (F - W)\tilde{x}. \tag{13}$$

From Theorem 2 in [25], we have  $\mathcal{R}_0^{av} < 1 \iff \sigma(F - W) < 0$ , where  $\sigma(M)$  is the stability modulus of the matrix  $M$  (i.e  $\sigma(M) = \max\{\text{Re } \nu, \nu \text{ an eigenvalue of } M\}$ ) and all the eigenvalues of  $F - W$  have negative real parts. Thus, the non-negative solutions of (13) are such that  $\lim_{t \rightarrow +\infty} \tilde{x}(t) = 0$ , or equivalently

$\lim_{t \rightarrow +\infty} \tilde{E}(t) = \lim_{t \rightarrow +\infty} \tilde{Q}(t) = \lim_{t \rightarrow +\infty} \tilde{C}(t) = \lim_{t \rightarrow +\infty} \tilde{I}_m(t) = \lim_{t \rightarrow +\infty} \tilde{I}_s(t) = \lim_{t \rightarrow +\infty} \tilde{H}(t) = \lim_{t \rightarrow +\infty} \tilde{L}(t) = \lim_{t \rightarrow +\infty} \tilde{R}(t) = \lim_{t \rightarrow +\infty} \tilde{V}(t) = 0$ . By the standard comparison principle [23] and the non-negativity of  $x$ , the nonnegative solutions of (5) satisfy  $\lim_{t \rightarrow +\infty} E(t) = \lim_{t \rightarrow +\infty} Q(t) = \lim_{t \rightarrow +\infty} C(t) = \lim_{t \rightarrow +\infty} I_m(t) = \lim_{t \rightarrow +\infty} I_s(t) = \lim_{t \rightarrow +\infty} H(t) = \lim_{t \rightarrow +\infty} L(t) = \lim_{t \rightarrow +\infty} R(t) = \lim_{t \rightarrow +\infty} V(t) = 0$ . Therefore, since  $\lim_{t \rightarrow +\infty} x(t) = 0$ , System (5) is an asymptotically autonomous system [2] (Theorem 2.5) with the limit system

$$\frac{d\bar{S}}{dt} = \Lambda - \mu\bar{S}. \tag{14}$$

It is obvious that the affine System (14) has a unique equilibrium given by  $S_0$ , which is GAS. This completes the proof.  $\square$

The GAS of the DFE for Model (5) when  $\mathcal{R}_0^{av}$  is less than one is illustrated in Figure 2.

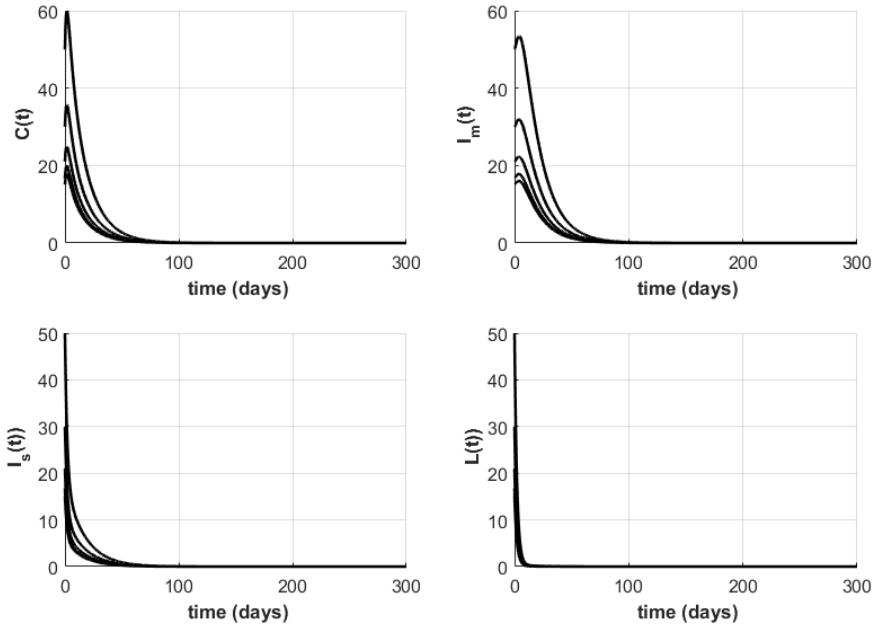


Figure 2: Stability of the DFE for Model (5) when  $\mathcal{R}_0^{av} < 1$ .

This figure is plotted with  $\beta_h = 0.25, \phi_2 = 0.1, \kappa_2 = 0.02949, \mu_v = 10.85, \mu = 14/350, \Lambda = 1000, 0221$ . The other parameters used are in Tables 2 and 3. With these parameters,  $\mathcal{R}_0^{av} = 0.4521$ .

### 3.5. Local stability of the endemic equilibrium

Now, we investigate the stability of the unique endemic equilibrium  $\mathcal{E}^*$ . Let  $\xi > 0$  be the non-negative real number such that  $\beta_v = \xi\beta_h$ , then the basic reproduction number  $\mathcal{R}_0^{av}$  becomes

$$\mathcal{R}_0^{av} = \frac{\beta_h [(b_1 d_4 d_2 d_7 d_5 + \varepsilon_1 K_2 d_2 d_7 d_5 + \varepsilon_2 K_3 + \varepsilon_3 K_5 d_5) \mu \mu_v + \xi \Lambda K_7]}{d_8 \mu \mu_v}$$

Let us consider that  $\mathcal{R}_0^{av} = 1$  and choose  $\beta_h$  as the bifurcation parameter.

Table 2: Fitted values to simulate Model (5).

Symbol	Value	Range	Symbol	Value	Range
$\Lambda$	100.0221	0–100	$\psi_1$	0.2501	0–1
$\psi_2$	0.0404	0–1	$\psi_3$	0.0569	0–1
$\chi$	0.5422	0–1	$\psi_4$	0.5379	0–1
$\beta_h$	0.4535	0–1	$\beta_v$	$3.08 \cdot 10^{-7}$	0–1
$p$	0.1342	0–1	$q$	0.0208	0–1
$\alpha$	0.0219	0–1	$\theta$	0.5252	0–1
$\phi_2$	0.6391	0–1	$\phi_1$	0.1420	0–1
$\delta$	0.4130	0–1	$\omega$	0.2720	0–1
$\sigma$	0.1743	0–1	$\eta$	0.0459	0–1
$f$	0.077	0–1	$\tau$	0.0633	0–1
$\kappa_1$	0.7348	0–1	$\kappa_2$	0.2949	0–1
$\varepsilon_1$	1.2008	0–2	$\varepsilon_2$	1.3160	0–2
$\varepsilon_3$	1.0028	0–2			

Table 3: Values in the litterature to simulate Model (5).

Symbol	Value	References	Range
$\mu$	14/1000	[1]	0–1
$\gamma$	1/7	[14]	0–1
$\mu_v$	0.85	[7]	0–1

The Jacobian matrix of System (5) at the DFE  $\mathcal{E}_0$  is given by:

$$J_{\beta^*}(\mathcal{E}_0) = \begin{pmatrix} -\mu & 0 & 0 & -\beta_h^* & -\varepsilon_1\beta_h^* & -\varepsilon_2\beta_h^* & 0 & -\varepsilon_3\beta_h^* & 0 & -\xi\beta_h^*\Lambda/\mu \\ 0 & -d_1 & 0 & \beta_h^* & \varepsilon_1\beta_h^* & \varepsilon_2\beta_h^* & 0 & \varepsilon_3\beta_h^* & 0 & \xi\beta_h^*\Lambda/\mu \\ 0 & 0 & -d_2 & 0 & \alpha & 0 & 0 & 0 & 0 & 0 \\ 0 & b_1 & 0 & -d_3 & 0 & 0 & 0 & 0 & 0 & 0 \\ 0 & b_2 & 0 & \phi_1 & -d_4 & 0 & 0 & 0 & 0 & 0 \\ 0 & b_3 & b_4 & 0 & \phi_2 & -d_5 & 0 & \delta & 0 & 0 \\ 0 & 0 & 0 & 0 & 0 & \theta & -d_6 & 0 & 0 & 0 \\ 0 & 0 & b_5 & 0 & 0 & 0 & 0 & -d_7 & 0 & 0 \\ 0 & 0 & b_6 & \kappa_1 & 0 & 0 & b_7 & \kappa_2 & -\mu & 0 \\ 0 & 0 & 0 & \psi_1 & \psi_2 & \psi_3 & 0 & \psi_4 & 0 & -\mu_v \end{pmatrix}.$$

System (5), with  $\beta_h = \beta_h^*$  has a nonhyperbolic equilibrium point (i.e the Jacobian matrix  $J_{\beta_h^*}$  has a simple eigenvalue with zero real part (here, zero is a simple eigenvalue), and the remaining eigenvalues have negative real parts). Therefore the Center Manifold Theory [3] (Theorem 4.1) can be applied to analyze the dynamics of System (5) near the bifurcation parameter  $\beta_h^*$ . It is easy to see that the components of a right-eigenvector of  $J_{\beta_h^*}$  associated to the zero eigenvalue  $w = (w_1, w_2, w_3, w_4, w_5, w_6, w_7, w_8, w_9, w_{10})^T$ , and the components of a left-eigenvector  $v = (v_1, v_2, v_3, v_4, v_5, v_6, v_7, v_8, v_9, v_{10})^T$  associated to zero would be given as

$$\left\{ \begin{array}{l} w_1 = -\frac{d_1 w_2}{\mu}, \\ w_2 = \frac{d_4 d_3 w_5}{b_1 \phi_1 + b_2 d_3}, \\ w_3 > 0, \\ w_4 = \frac{b_1 d_4 w_5}{b_1 \phi_1 + b_2 d_3}, \\ w_5 = \frac{d_2 w_3}{\alpha}, \\ w_6 = \frac{b_3 w_2 + b_4 w_3 + \phi_2 w_5 + \delta w_8}{d_5}, \\ w_7 = \frac{\theta w_6}{d_6}, \\ w_8 = \frac{b_5 w_3}{d_7}, \\ w_9 = \frac{b_6 w_3 + \kappa_1 w_4 + b_7 w_6 + \kappa_2 w_7}{\mu}, \\ w_{10} = \frac{\psi_1 w_4 + \psi_2 w_5 + \psi_3 w_6 + \psi_4 w_8}{\mu_v}, \end{array} \right. \quad \text{and} \quad \left\{ \begin{array}{l} v_1 = 0, \\ v_2 = \frac{b_1 v_4 + b_2 v_5 + b_3 v_6}{d_1}, \\ v_3 = \frac{b_4 v_6 + b_5 v_8}{d_2}, \\ v_4 = \frac{\beta_h v_2 + \phi_1 v_5}{d_3}, \\ v_5 = \frac{\varepsilon_1 \beta_h v_2 + \alpha v_3 + \phi_2 v_6}{d_4}, \\ v_6 = \frac{\varepsilon_2 \beta_h v_2 + \theta v_7}{d_5}, \\ v_7 = 0, \\ v_8 = \frac{\varepsilon_3 \beta_h v_2 + \delta v_6}{d_7}, \\ v_9 = 0, \\ v_{10} = \frac{\xi \beta_h \Lambda v_2}{\mu \mu_v}. \end{array} \right.$$

Using the result from Castillo-Chavez et al. [3] (Theorem 4.1), we calcu-



late the coefficients  $\mathcal{A}$  and  $\mathcal{B}$  as

$$\mathcal{A} = -2v_2 \left( \frac{d_1 w_2}{\mu} w_{10} \xi \beta_h + \frac{\beta_h \mu}{\Lambda} \right) (w_4 + \varepsilon_1 w_5 + \varepsilon_2 w_6 + \varepsilon_3 w_8) \cdot (w_2 + w_4 + w_5 + w_6 + w_8 + w_9) < 0$$

and

$$\mathcal{B} = v_2 \left( w_4 + \varepsilon_1 w_5 + \varepsilon_2 w_6 + \varepsilon_3 w_8 + \frac{\xi \Lambda}{\mu} w_{10} \right) > 0.$$

Hence by the theorem of Castillo-Chavez et al. [3] (Theorem 4.1), one has the result.

**THEOREM 3.6** If  $\mathcal{R}_0^{av} > 1$ , then System (5) undergoes a trans-critical bifurcation with  $\mathcal{R}_0^{av} = 1$  being the bifurcation parameter, that is when  $\mathcal{R}_0^{av}$  changes from values less, but close to one to the values greater than one, the DFE changes its stability from stable to unstable, and in this case, the unique endemic equilibrium  $\mathcal{E}^*$  becomes LAS.

The stability of the endemic equilibrium for Model (5) is illustrated in Figure 3. This figure suggests the global asymptotic stability of this equilibrium whenever  $\mathcal{R}_0^{av}$  is greater than one.

**4. Sensitivity analysis** The sensitivity analysis is performed to assess the impact of variation of parameters in the prediction of the model. In this section, we consider all the parameters as uncertain, but belonging to the ranges given in Tables 2 and 3. The Latin hypercube sampling (LHS) samples 1000 values for each parameter using the uniform distribution and the Partial Rank Correlation Coefficients (PRCC) as well as the  $p$ -values are computed for the total number of infected  $C + Q + H + I_s + I_m + L$ . The obtained result is presented in Figure 4. In this work, we decide that a parameter is significant if its PRCC value is greater or less than 0.05 and its  $p$ -value less than 0.05, meaning that there is less than 5% of chance that the results being random. According to Figure 4, the most significant parameters which contribute in an increasing number of infected when their values increase are respectively  $\beta_v, \beta_h$  and  $\delta$ . This shows that reducing the environment/human to human transmission is of paramount importance to mitigate the spread of COVID-19. This could be achieved through disinfection, social distancing, lockdown, etc. On the contrary, the natural mortality, the mortality due to disease and the recovery rates are the most influential parameters which decrease the number of infected whenever they increase. The sensitivity analysis in particular highlights the usefulness of isolation and self-isolation in reducing the number of COVID-19 infected. Moreover, it shows that the escape from isolation  $f$  has a negative impact on the dynamics of the disease, but it is not a highly influential parameter.

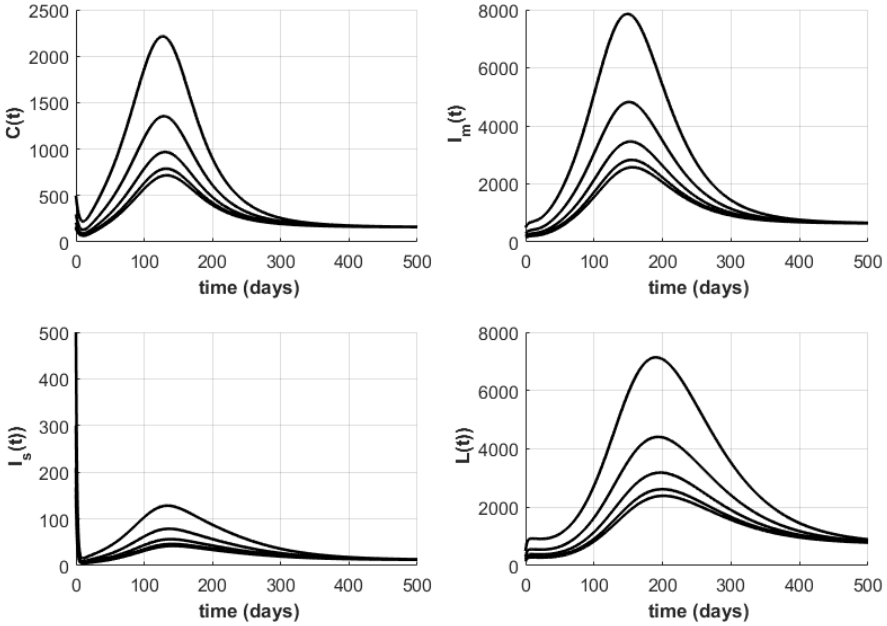


Figure 3: Stability of the endemic equilibrium for Model (5).

This figure is plotted with  $\psi_1 = 0.002501, \psi_2 = 0.0000404, \psi_3 = 0.0000569, \psi_4 = 0.0005379, \gamma = 0.008, \beta_h = 0.24535, \phi_2 = 0.0006391, \theta = 0.05252, \delta = 0.004130, \eta = 0.459, f = 1, \kappa_1 = 0.0007348, \kappa_2 = 0.0002949$ . The other parameters used are in Tables 2 and 3. With these parameters,  $\mathcal{R}_0^{av} = 5.0559$ .

**5. Numerical simulations: Case study of Rwanda** Some simulations are carried out in this section in order to support the mathematical results, to validate our model and provide a short forecast of the ongoing epidemic. The model is fitted to the number of asymptomatic reported cases in Rwanda from 1 April, 2022 to 15 June, 2022 [22]. We choose the number of asymptomatic cases for the calibration process because, according to Model (5), the symptomatic infected cases are split into several compartments ( $I_s, I_m, L, H, \dots$ ) of which the data are not available (only the total data for symptomatic cases are provided). Note that the greatest proportion of COVID-19 cases are asymptomatic, so, this class of infected is a serious matter and their control is of paramount importance as far as reducing the spread of COVID-19 is concerned.

**5.1. Model validation** For the validation of the model, we fit the cumulative cases of asymptomatic individuals during the period of the 1 April, 2022 to the 15 June, 2022, using the Nonlinear Least Squares Fitting Method.

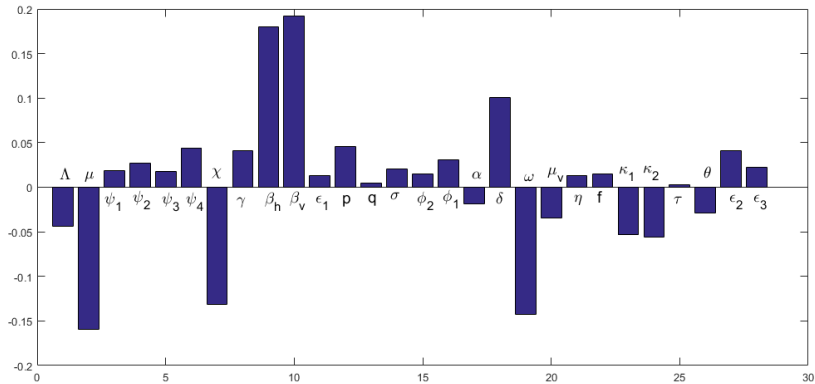


Figure 4: PRCCs of the  $C + Q + H + I_s + I_m + L$ .

Thanks to [21], the total population of Rwanda is estimated to 13, 776, 698. But on the 1 April 2022, only one infected person was in isolation and 4 cases were reported this day. Among these cases, 3 were asymptomatic. Thus, we consider the initial condition:  $S(0) = 13, 776, 693; E(0) = Q(0) = I_s(0) = L(0) = R(0) = V(0) = 0; C(0) = 3; I_m(0) = 1; H(0) = 1$ . Moreover, the number of cumulative asymptomatic cases displayed in Table 5 are computed using the daily number of asymptomatic cases reported in [22]. The fitted parameters are given in Table 2 and the corresponding fitted curve is plotted in Figure 5(a). In order to assess the accuracy of our predictions, we calculate two performance metrics: The Mean Absolute Error (MAE) and the Root Mean Square Error (RMSE), which are defined as follows [14]:

$$MAE = \frac{1}{N_p} \sum_{i=1}^{N_p} |Y(i) - \hat{Y}(i)| \text{ and } RMSE = \sqrt{\frac{\sum_{i=1}^{N_p} (Y(i) - \hat{Y}(i))^2}{N_p}},$$

where  $Y(i)$  represents original cases,  $\hat{Y}(i)$  are predicted values and  $N_p$  is the size of the data. The computation of these metrics gives:  $MAE = 0.0962$  and  $RMSE = 0.8332$ . These small values, in conjunction with Figure 5(a) show that our model performs excellently the dynamics of COVID-19 in Rwanda and can be therefore used to forecast the outcome of the pandemic in this country. With the estimated values, one has  $\mathcal{R}_0^h = 0.6485$  and  $\mathcal{R}_0^v = 6.8521 \cdot 10^{-4}$ . Thus, the contribution of the environmental transmission to the basic reproduction number is negligible in Rwanda. This is in accordance with the results found in [17]. However, the impact of the environmental transmission is not negligible in every country, see for instance [7] and the references

therein. The value of  $\mathcal{R}_0^{av}$  obtained shows that the COVID-19 is expected to disappear without any additional control measure in Rwanda, especially if its dynamics does not exhibit a backward bifurcation phenomenon as it is the case for our model.

The curves of the infectious compartments plotted in Figure 5(b) emphasize that the great number of infectious are asymptomatic in Rwanda as found in [11], followed by the individuals who exhibit severe symptoms of the disease. These curves also highlight that the infected in Rwanda do not practically escape from the self-isolation. The latter outcome may explain the few number of cases reported in Rwanda and supports the good management of infected individuals in this country [16].

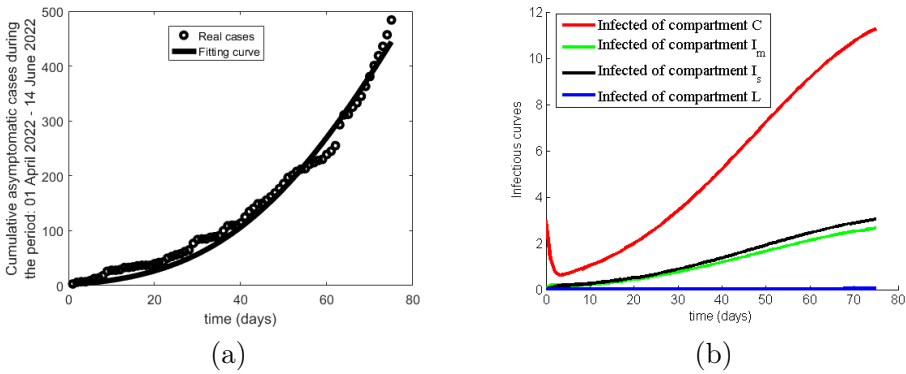


Figure 5: Fitting curve.

The first figure fits the cumulative number of asymptomatic cases in Rwanda and the second figure plots the dynamics of the infectious compartments. The parameters used are gathered in Tables 2 and 3.

**5.2. Long-time behaviour of the outbreak in Rwanda** From Figure 5, one has the impression that the cumulative number of asymptomatic cases as well as the number of infected who belong to the compartments  $C$ ,  $I_m$  and  $I_s$  increase as the time evolves. But, since the value of the basic reproduction number is less than one, the disease would disappear. In Figure 6, we forecast the number of infected in the long run (300 days). According to this figure, the COVID-19 would have disappeared in Rwanda at the beginning of the year 2023. But, actually, a few number of cases continue to be registered in this country [8]. This would be attributed to the migration of infected, not taken into account in the model formulation. We however hope that this aspect will only postpone the end of the outbreak and would not greatly influence the end of the outbreak in the long run.

**5.3. Usefulness of isolation and self-isolation** The isolation measure is a well known control strategy in epidemiology to contain the infectious

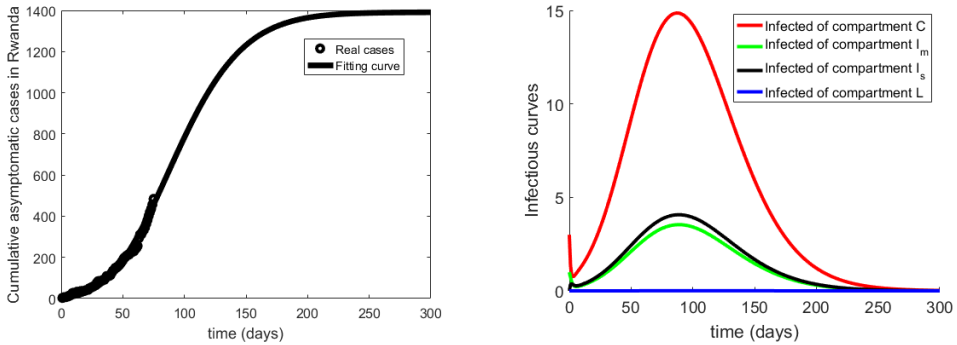


Figure 6: Solution of the model in Rwanda up to 10 months and dynamics of the infectious compartment of Model (5). All the parameters used are gathered in Tables 2 and 3.

illnesses. For COVID-19, so that the centres of isolation are not overflowed and because of what most cases endure a benign shape of the illness, the self-isolation has been experimented as an another control strategy. In this project, we have supposed the isolation and the self-isolation to be effective, in the sense that the isolated and the self-isolated people don't transmit the illness. This assumption seems realistic for the case of Rwanda, since the Rwanda government took strong mitigation measures for a good management of infected cases and to increase the awareness of the population [16]. In this paragraph, we investigate the impact of these control strategies by changing the values of the parameter  $\alpha$  of the self-isolation and secondly the parameter  $\theta$  of the isolation. Thus, we construct in Figure 7 the curves of infectious with the initial conditions and the parameters estimated in Rwanda. These curves show that the number of infectious in the compartments,  $C, I_m$  and  $I_s$  are decreasing functions of  $\alpha$  and  $\theta$ . Table 4 comforts the fact that increasing  $\alpha$  and  $\theta$  decreases the level of the pandemic. In particular, one observes that the isolation has bigger impact on the number of infected and on the basic reproduction number than the self-isolation measure. This figure corroborates the importance of the isolation and the self-isolation to reduce the spread of COVID-19.

Table 4: Values of  $\mathcal{R}_0^h$  and  $\mathcal{R}_0^v$  when the parameters  $\alpha$  and  $\theta$  vary.

	$\alpha = 0.05$	$\alpha = 0.1$	$\alpha = 0.2$	$\theta = 0.05$	$\theta = 0.1$	$\theta = 0.2$
$\mathcal{R}_0^h$	0.6427	0.6345	0.6210	0.7592	0.7399	0.7090
$\mathcal{R}_0^v$	$6.8214 \cdot 10^{-4}$	$6.7725 \cdot 10^{-4}$	$6.6918 \cdot 10^{-4}$	$7.1273 \cdot 10^{-4}$	$7.0796 \cdot 10^{-4}$	$7.0031 \cdot 10^{-4}$

**5.4. Impact of the environmental transmission** The validation of the model done in Section 5.1 highlighted that the environmental transmission of the COVID-19 is not too important in Rwanda, practically negligible. This

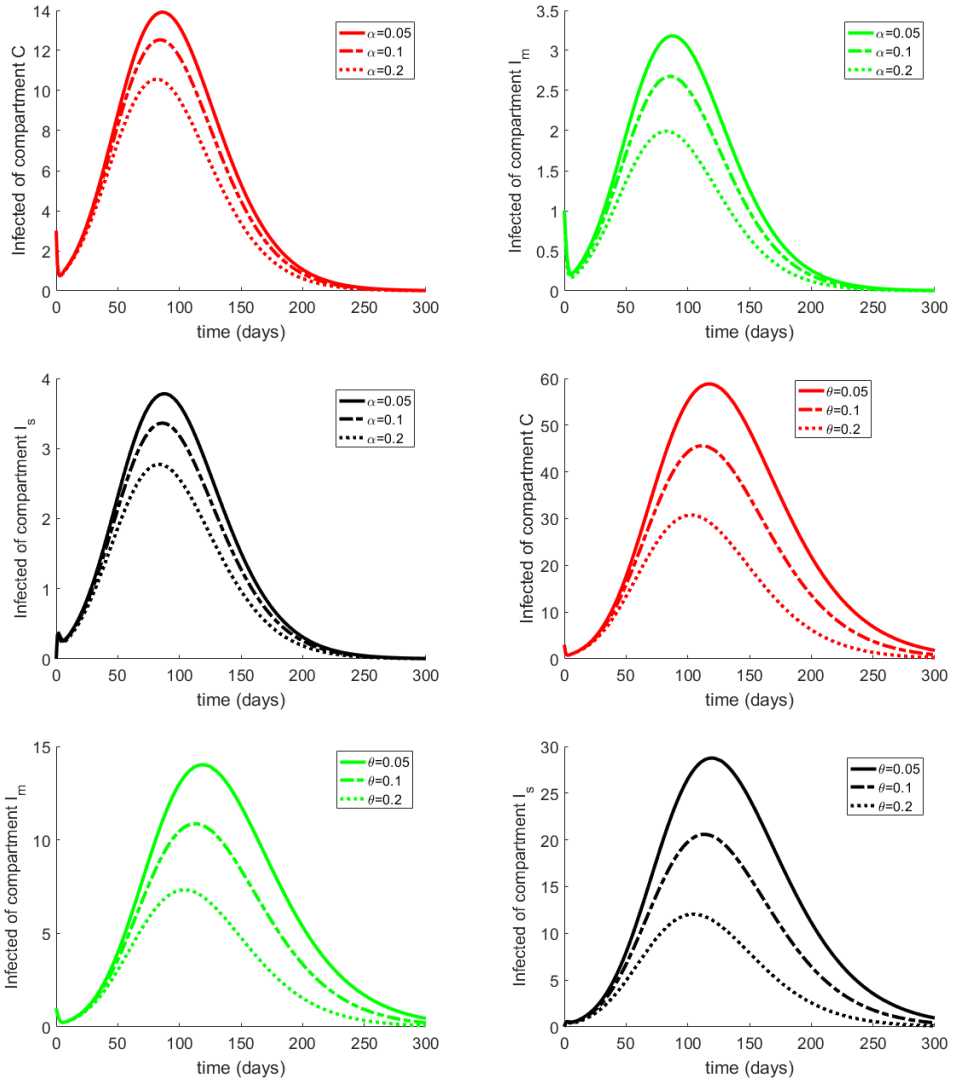


Figure 7: Usefulness of isolation and self-isolation measure.

This figure is plotted for (i)  $\alpha = 0.05$ ;  $\alpha = 0.1$  and  $\alpha = 0.2$ ; (ii)  $\theta = 0.05$ ;  $\theta = 0.1$  and  $\theta = 0.2$ . The other parameters are in Tables 2 and 3. It emphasizes the sensitivity of  $\alpha$  and  $\theta$ .

is caused by the adherence of people to barrier measures (regular washing of the hands; the wearing of mufflers,...) in the country at that particular time of the pandemic [16]. However, in spite of the poor contribution of the environmental transmission to the basic reproduction number, one should remember that  $\beta_v$  highly influences the number of COVID-19 infected cases, as found in Section 4. This result was expected, because the environmental transmission was modelled like a mass action transmission, which is supported

by several studies [7, 19]. In this section, we want to illustrate how a few change in the value of  $\beta_v$  would influence the number of COVID-19 infected cases. We consider three values of  $\beta_v$ :  $3 \cdot 10^{-7}$ ,  $3.04 \cdot 10^{-7}$  and  $3.08 \cdot 10^{-7}$ . The curves of the corresponding number of infected are plotted in Figure 8. One can see that although the environmental transmission does not have a significant contribution on the basic reproduction number,  $\beta_v$  has a noticeable impact on the peak of the epidemic.

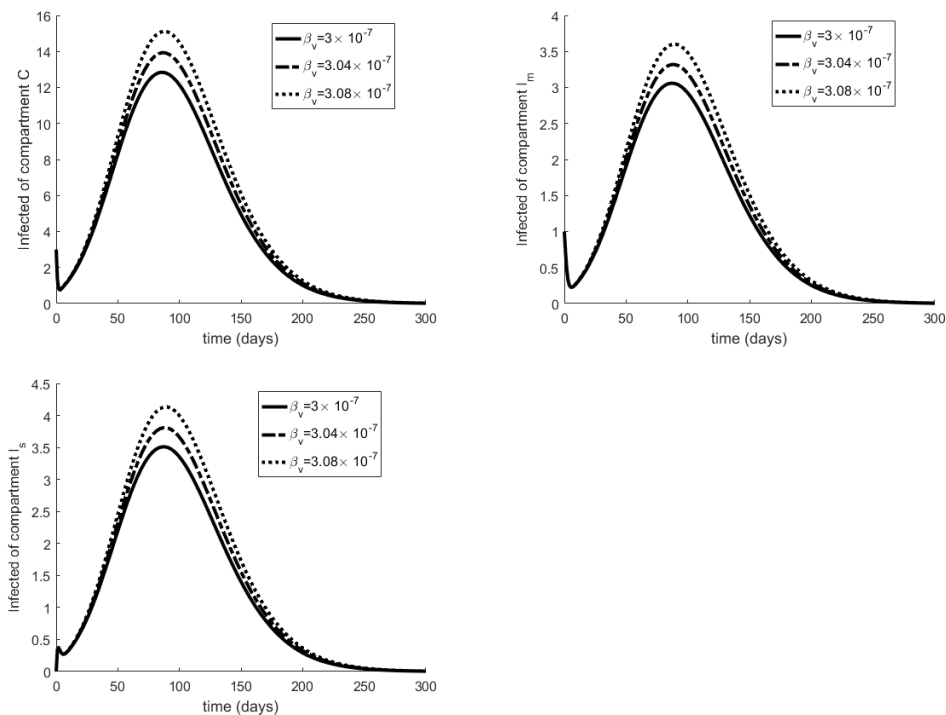


Figure 8: Impact of the environmental transmission.

This figure is plotted for (i)  $\beta_v = 3 \cdot 10^{-7}$  (solid line) and for (ii)  $\beta_v = 3.04 \cdot 10^{-7}$  (dash line), (iii)  $\beta_v = 3.08 \cdot 10^{-7}$  (dotted line). The other parameters are in Tables 2 and 3.

**5.5. Investigating the impact of the individuals who escape from the self-isolation** Until now, we did not investigate numerically the impact of the individuals who do not comply to the self-isolation measure. This is addressed in this paragraph, by taking  $L(0) = 10$  the other values of the initial condition remain the same. We investigate the dynamics of the infected when  $f$  varies. We suppose (i)  $f = 0.05$ , (ii)  $f = 0.5$  and (iii)  $f = 0.9$ . Figure 9 shows that when  $f$  increases, the number of infected increases as well, but the impact of  $f$  is very weak. This figure suggests that the fact that some infected don't comply to the self-isolation cannot be relevant to justify the

persistence or the endemicity of COVID-19.

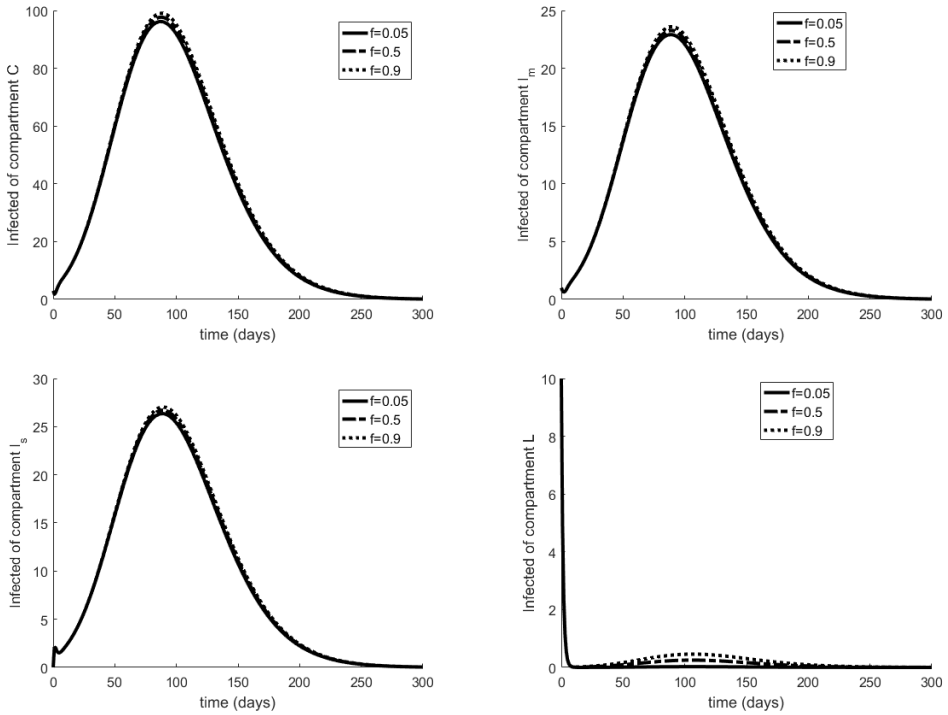


Figure 9: Impact of the individuals who escape from the self-isolation. This figure is plotted for (i)  $f = 0.05$ , (ii)  $f = 0.5$  and (iii)  $f = 0.9$ . The other parameters are in Tables 2 and 3. This figure shows the weak sensitivity of  $f$ .

**6. Conclusion** Since the beginning of the outbreak of COVID-19 in December 2019, more than several protocols and model was developed.

In this paper, we proposed a model which focused on two control strategies: the isolation and the self-isolation of infected cases. Indeed so that medical center are not overwhelmed, countries with a great number of cases implemented the self-isolation measure of infected showing benign symptoms. The mathematical analysis of the model has been provided. The main results are summarized as follows:

- The model always admits a DFE, which is GAS when the basic reproduction number  $\mathcal{R}_0^{av}$  is less than one.
- When the basic reproduction number is greater than one, we have proved that the model admits a unique endemic equilibrium, which is LAS.

The sensitivity analysis of the model has been done. This analysis has shown



the high impact of both human to human and environment to human transmissions on the number of COVID-19 infected cases and has highlighted the usefulness of disinfection, isolation and self-isolation to mitigate the spread of the disease. Numerical simulations have been addressed to support theoretical and sensitivity analysis. Both these analyses have shown that the escapers from isolation do not contribute a lot to the spread of the disease and this fact should not explain or justify the persistence of COVID-19. Numerically, we fitted the model to the daily cumulative asymptomatic cases in Rwanda reported during the period: 1 April 2022 to 14 June 2022. With the obtained parameters, we have found  $\mathcal{R}_0^{av} = 0.6485 < 1$ . Thus, the epidemic will be overcome in Rwanda. We have shown moreover that most number of cases in Rwanda are asymptomatic infected cases, which is in line with the previously study done in [11]. Furthermore, the solution of the model plotted up to 10 months have shown that towards the beginning of the year 2023, the number of cases would be practically zero. Thus, according to our prevision, the COVID-19 would have disappeared in Rwanda at the beginning of the year 2023. This outcome does not exactly reflect the reality, but is very close to that (see the reference [8] for instance). The little gap between this prediction and the reality could be attributed to two main reasons:

- The migration of infected cases has not been taken into account in the model formulation;
- The number of asymptomatic cases has been calibrated instead of the number of symptomatic cases;

Obviously, the number of asymptomatic reported cases would be underestimated. However, we chose to calibrate this number instead of the symptomatic cases because our model split the symptomatic cases into several compartments (moderate, severe, hospitalized patients, . . .), from which the data are not available.

Almost all the models developed until now to understand the spread of the COVID-19 pandemic forecast a catastrophic impact of the illness world wide. Indeed, according to the basic reproduction number previously reported [14, 17, 18, 24, 27], the COVID-19 would persist and would become endemic. A previous study [15] addressed to assess the knowledge, attitudes and preventive practices against COVID-19 in Rwanda showed that the population were aware about the disease and agreed the necessity of self-isolation, social distancing, hand washing, the using of faces masks and gloves, . . . Moreover, in this country, the self-isolated patients were closely observed and managed while they remained in their homes [16]. Rwanda is one of a few countries that have quickly adopted and implemented strong mitigation measures, and progressive capacity building to fight against COVID-19. These facts may explain the elimination of the disease in this country and its lesser impact.

The model we have considered in this paper, has involved several com-

partments, making the interpretation of the results a bit difficult. This is due to the fact that some control measures (self-isolation, isolation), different status of infected individuals (asymptomatic, moderate infected, severe infected, escapers from the isolation, . . .) and different transmission routes (human to human and environment to human), have been taken into account together. In our future project, we are going to focus on few aspects of this study to better highlight their impact on the dynamics of the disease.

Moreover, how can we understand the lesser impact of COVID-19 in Africa (in general), which has a poor medical/communication system and a great number of populations (in some countries) who have misconceptions (deny, attribute it to witchcraft, . . .) about COVID-19 [13]? This other perspective is actually the focus of our investigations.

**Author Contributions:** All authors equally contributed to the conceptualization, methodology, formal analysis, investigation, and writing—original draft preparation.

**Funding:** This research received no external funding. Polish Mathematical Society remains neutral regarding jurisdictional claims in published maps and institutional affiliations.

**Conflicts of Interest:** The authors declare no conflict of interest.

**Acknowledgments:** The authors would like to thank the reviewers and editor for their valuable comments and suggestions for the improvement of this paper.

## References

- [1] I. Area, F. Ndairou, J. J. Nieto, C. J. Silva, and D. F. Torres. Ebola model and optimal control with vaccination constraints. *Journal of Industrial and Management Optimization*, 14(2):427–446, 2018. ISSN 1547-5816. doi: [10.3934/jimo.2017054](https://doi.org/10.3934/jimo.2017054). Cited on p. 253.
- [2] O. Arino, D. Axelrod, M. Kimmel, and M. Langlais. *Mathematical population dynamics: analysis of heterogeneity*. Berlin, 1995. Cited on p. 251.
- [3] C. Castillo-Chavez and B. Song. Dynamical models of tuberculosis and their applications. *Mathematical Biosciences & Engineering*, 1(2):361–404, 2004. ISSN 1551-0018. doi: [10.3934/mbe.2004.1.361](https://doi.org/10.3934/mbe.2004.1.361). Cited on pp. 254 and 255.
- [4] Coronavirus. Coronavirus (COVID-19) dashboard. WHO, 2023. <https://covid19.who.int/>. Last Access 08 July 2023. Cited on p. 240.
- [5] Coronavirus disease. Coronavirus disease (covid-19): how is it transmitted? WHO, 2021. URL <https://www.who.int/news-room/questions-and-answers/item/coronavirus-disease-covid-19-how-is-it-transmitted>. Last access 08, July 2023. Cited on p. 240.
- [6] O. Diekmann, J. Heesterbeek, and M. G. Roberts. The construction of next-generation matrices for compartmental epidemic models. *Journal of the Royal Society Interface*, 7(47):873–885, 2010. doi: [10.1098/rsif.2009.0386](https://doi.org/10.1098/rsif.2009.0386). Cited on p. 240.

- 
- [7] S. M. Garba, J. M.-S. Lubuma, and B. Tsanou. Modeling the transmission dynamics of the covid-19 pandemic in south africa. *Mathematical Biosciences*, 328:108441, 2020. doi: [10.1016/j.mbs.2020.108441](https://doi.org/10.1016/j.mbs.2020.108441). Cited on pp. 241, 242, 253, 257, and 261.
- [8] Global. Global Rwanda situation. WHO, 2019. URL <https://covid19.who.int/region/afro/country/rw>. Last access 08, July 2023. Cited on pp. 258 and 263.
- [9] Isolation. Isolation and precautions for people with COVID-19. CDC, 2023. <https://www.cdc.gov/coronavirus/2019-ncov/your-health/isolation.html>. Last Access 08 July 2023. Cited on p. 240.
- [10] B. Ivorra, M. R. Ferrández, M. Vela-Pérez, and A. M. Ramos. Mathematical modeling of the spread of the coronavirus disease 2019 (covid-19) taking into account the undetected infections. the case of china. *Communications in Nonlinear Science and Numerical Simulation*, 88:105303, 2020. ISSN 1007-5704. doi: [10.1016/j.cnsns.2020.105303](https://doi.org/10.1016/j.cnsns.2020.105303). Cited on p. 240.
- [11] N. Karim et al. Lessons learned from rwanda: innovative strategies for prevention and containment of covid-19. *Annals of Global Health*, 87(1), 2021. doi: [10.5334/aogh.3172](https://doi.org/10.5334/aogh.3172). Cited on pp. 258 and 263.
- [12] M. Massard, R. Eftimie, A. Perasso, and B. Saussereau. A multi-strain epidemic model for covid-19 with infected and asymptomatic cases: application to french data. *Journal of Theoretical Biology*, 545:111117, 2022. ISSN 0022–5193. doi: [10.1016/j.jtbi.2022.111117](https://doi.org/10.1016/j.jtbi.2022.111117). Cited on p. 242.
- [13] P. M. Mphekgwana, M. M, and T. M. Mothiba. Use of traditional medicines to fight covid-19 during the south african nationwide lockdown: a prevalence study among university students and academic staff. *The Open Public Health Journal*, 14:441–445, 2021. doi: [10.2174/1874944502114010441](https://doi.org/10.2174/1874944502114010441). Cited on p. 264.
- [14] S. S. Nadim, I. Ghosh, and J. Chattopadhyay. Short-term predictions and prevention strategies for covid-19: a model-based study. *Applied Mathematics and Computation*, 404:126251, 2021. doi: [10.1016/j.amc.2021.126251](https://doi.org/10.1016/j.amc.2021.126251). Cited on pp. 253, 257, and 263.
- [15] P. Ndishimye et al. Knowledge, attitudes and preventive practices towards covid-19 among frontline healthcare workers in rwanda. *Rwanda Public Health Bulletin*, 2(1):16–21, 2020. Cited on p. 263.
- [16] M. Nkeshimana et al. Experience of rwanda on covid-19 case management: from uncertainties to the era of neutralizing monoclonal antibodies. *International Journal of Environmental Research and Public Health*, 19(3):1023, 2022. doi: [10.3390/ijerph19031023](https://doi.org/10.3390/ijerph19031023). Cited on pp. 258, 259, 260, and 263.
- [17] C. H. Nkwayep, S. Bowong, J. Tewa, and J. Kurths. Short-term forecasts

- of the covid-19 pandemic: a study case of cameroon. *Chaos, Solitons & Fractals*, 140:110106, 2020. doi: [10.1016/j.chaos.2020.110106](https://doi.org/10.1016/j.chaos.2020.110106). Cited on pp. 257 and 263.
- [18] C. H. Nkwayep, S. Bowong, B. Tsanou, M. A. Alaoui, and J. Kurths. Mathematical modeling of covid-19 pandemic in the context of sub-saharan africa: a short-term forecasting in cameroon and gabon. *Mathematical Medicine and Biology: A Journal of the IMA*, 39(1):1–48, 2022. doi: [10.1093/imammb/dqab020](https://doi.org/10.1093/imammb/dqab020). Cited on pp. 240 and 263.
- [19] A. J. Ouemba Tassé, B. Tsanou, J. Lubuma, J. L. Woukeng, and F. Signing. Ebola virus disease dynamics with some preventive measures: a case study of the 2018–2020 kivu outbreak. *Journal of Biological Systems*, 30 (01):113–148, 2022. doi: [10.1016/j.amsu.2022.104213](https://doi.org/10.1016/j.amsu.2022.104213). Cited on p. 261.
- [20] T. Piasecki, P. B. Mucha, and M. Rosińska. On limits of contact tracing in epidemic control. *Plos One*, 16(8):e0256180, 2021. doi: [10.1371/journal.pone.0256180](https://doi.org/10.1371/journal.pone.0256180). Cited on p. 240.
- [21] Rwanda. Rwanda population growth rate 1950-2023. Macrotrends, 2023. URL <https://www.macrotrends.net/countries/RWA/rwanda/population-growth-rate/>. Cited on p. 257.
- [22] Situation. Situation report on-COVID-19 in rwanda, 2019. URL <https://www.rbc.gov.rw/index.php?id=717>. Cited on pp. 256 and 257.
- [23] H. L. Smith and P. Waltman. *The theory of the chemostat: dynamics of microbial competition*, volume 13. Cambridge University Press, 1995. Cited on p. 251.
- [24] C. Tadmon and S. Foko. A transmission dynamics model of covid-19: case of cameroon. *Infectious Disease Modelling*, 7(2):211–249, 2022. doi: [10.1016/j.idm.2022.05.002](https://doi.org/10.1016/j.idm.2022.05.002). Cited on p. 263.
- [25] P. Van den Driessche and J. Watmough. Reproduction numbers and sub-threshold endemic equilibria for compartmental models of disease transmission. *Mathematical Biosciences*, 180(1-2):29–48, 2002. doi: [10.1016/s0025-5564\(02\)00108-6](https://doi.org/10.1016/s0025-5564(02)00108-6). Cited on pp. 247, 249, and 251.
- [26] Z. Wu and J. M. McGoogan. Characteristics of and important lessons from the coronavirus disease 2019 (covid-19) outbreak in china: summary of a report of 72 314 cases from the chinese center for disease control and prevention. *JAMA*, 323(13):1239–1242, 2020. doi:[10.1001/jama.2020.2648](https://doi.org/10.1001/jama.2020.2648). Cited on p. 240.
- [27] C. Yang and J. Wang. A mathematical model for the novel coronavirus epidemic in wuhan, china. *Mathematical Biosciences and Engineering*, 17(3):2708, 2020. doi: [10.3934/mbe.2020148](https://doi.org/10.3934/mbe.2020148). Cited on p. 263.

## Appendices

### A. Proof of Theorem 3.1. Let

$$T = \sup\{t > 0/\forall z \in [0, t] : (S(z), E(z), Q(z), C(z), I_m(z), I_s(z), H(z), L(z), R(z), V(z)) \geq 0\}.$$

By the definition of  $T$ , it follows that  $T > 0$ .

To show that  $S(t) > 0$  for all  $t \geq 0$ , we only need to prove that  $S(T) > 0$ . It follows from the first equation of System (5) that

$$\frac{dS}{dt} = \Lambda - [\mu + \lambda(t)], \quad \text{where } \lambda(t) \text{ is given by the Eq. (4).} \tag{15}$$

Thus,

$$\frac{d}{dt} \left[ S(t) \exp \left( \int_0^t \lambda(s) ds + \mu t \right) \right] = \Lambda \exp \left( \int_0^t \lambda(s) ds + \mu t \right),$$

Integrating the above equation from 0 to  $T$  gives

$$S(T) \exp \left( \int_0^T \lambda(s) ds + \mu T \right) - S(0) = \int_0^T \left\{ \Lambda \exp \left( \int_0^t \lambda(s) ds + \mu t \right) \right\} dt.$$

The multiplication of both sides of the equation above by

$$\exp \left( -\mu T - \int_0^T \lambda_h(s) ds \right) \text{ yields}$$

$$\begin{aligned} S(T) &= \left[ S(0) + \int_0^T \left\{ \Lambda \exp \left( \int_0^t \lambda(s) ds + \mu t \right) \right\} dt \right] \\ &\quad \cdot \exp \left( -\mu T - \int_0^T \lambda(s) ds \right) > 0. \end{aligned}$$

From this, we deduce that  $S(T) > 0$ , and thus  $S(t) > 0$  for all  $t \geq 0$ .

To prove the positivity of the other variables, we use the tangent condition. According to [? ], we need to show that  $\langle n(x)|g(x) \rangle \leq 0$ , for  $x$  on each of the hyperplane  $E = Q = C = I_m = I_s = H = L = R = V = 0$  of  $\mathbb{R}^9$ ;  $n$  is the outer normal vector to the hyperplane and  $g(x)$  is the vector field defined by the right-hand side of System (5) except the equation for  $S$ .

For the hyperplane  $E = 0$ , we have  $n(x) = (-1, 0, 0, 0, 0, 0, 0, 0, 0)$ . This gives:

$$\langle n(x)|g(x) \rangle = -\frac{\beta_h(C + \varepsilon_1 I_m + \varepsilon_2 I_s + \varepsilon_3 L)S}{N - Q - H} - \beta_v V S \leq 0.$$

So the tangent condition is verified.

Moreover,

$$\frac{dE}{dt} = \frac{\beta_h(C + \varepsilon_1 I_m + \varepsilon_2 I_s + \varepsilon_3 L)S}{N - Q - H} + \beta_v V S \geq 0, \quad (16)$$

since we are in the non-negative orthant. Similarly, it can be proved using the other hyperplanes that  $\langle n(x)|g(x) \rangle \leq 0$  and  $dA/dt \geq 0$ ,  $A \in \{Q, C, I_m, I_s, H, L, R, V\}$ . Hence, the other variables of the model are positive.

Furthermore, by adding the first nine equations of System (5), we have:

$$\frac{dN(t)}{dt} = \Lambda - \mu N - \chi I_s - \sigma \omega H \leq \Lambda - \mu N. \quad (17)$$

The Gronwall's inequality applied to (17) gives

$$N(t) \leq \frac{\Lambda}{\mu} + \left( N(0) - \frac{\Lambda}{\mu} \right) \exp(-\mu t), \quad \forall t \geq 0.$$

Therefore, if  $N(0) \leq \frac{\Lambda}{\mu}$ , then for every  $t \geq 0$ ,  $0 \leq N(t) \leq \frac{\Lambda}{\mu}$ .

Finally, with the assumption  $N(t) \leq \frac{\Lambda}{\mu}$ , and using the fact  $C(t) \leq N(t)$ ,  $I_m(t) \leq N(t)$ ,  $I_s(t) \leq N(t)$ ,  $L(t) \leq N(t)$ , applying the Gronwall inequality once more, one gets for every  $t \geq 0$

$$V(t) \leq \frac{\Lambda(\psi_1 + \psi_2 + \psi_3 + \psi_4)}{\mu_v \mu}, \quad \text{whenever } V(0) \leq \frac{\Lambda(\psi_1 + \psi_2 + \psi_3 + \psi_4)}{\mu_v \mu}.$$

## B. Table of asymptomatic cases in Rwanda

Table 5: Asymptomatic cases in Rwanda during the period: 01.04.2022 to 14.06.2022 (Asymp. stands for Asymptomatic, Cum. stands for cumulative).

Dates	Asymp. cases	Cum. asymp. cases	Dates	Asymp. cases	Cum. asymp. cases
01-04	3	3	09-05	0	110
02-04	3	6	10-05	4	114
03-04	1	7	11-05	11	125
04-04	0	7	12-05	10	135
05-04	2	9	13-05	6	141
06-04	4	13	14-05	8	149
07-04	1	14	15-05	1	150
08-04	4	18	16-05	6	156
09-04	8	26	17-05	6	162

10-04	2	28	18-05	3	169
11-04	0	28	19-05	8	177
12-04	1	29	20-05	9	186
13-04	4	33	21-05	11	197
14-04	0	33	22-05	4	201
15-04	1	34	23-05	7	208
16-04	2	36	24-05	4	212
17-04	1	37	25-05	1	213
18-04	0	37	26-05	8	221
19-04	0	37	27-05	3	224
20-04	3	40	28-05	4	228
21-04	2	42	29-05	2	230
22-04	1	43	30-05	9	239
23-04	7	50	31-05	6	245
24-04	3	53	01-06	10	255
25-04	3	56	02-06	38	293
26-04	2	58	03-06	18	311
27-04	4	62	04-06	1	312
28-04	3	65	05-06	13	325
29-04	12	77	06-06	8	333
30-04	7	84	07-06	12	345
01-05	1	85	08-06	18	363
02-05	0	85	09-06	18	381
03-05	3	88	10-06	20	401
04-05	1	89	11-06	18	419
05-05	2	91	12-06	17	436
06-05	9	100	13-06	21	457
07-05	9	109	14-06	27	484
08-05	1	110			

**Badanie wpływu izolacji, samoizolacji i transmisji  
środowiskowej na rozprzestrzenianie się COVID-19:  
Studium przypadku w Rwandzie**

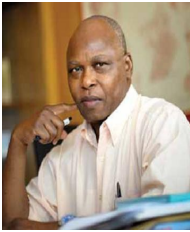
Jean Lubuma, Arsène Jaures Ouemba Tassé, Francis Signing, Berge Tsanou

**Streszczenie** W niniejszej pracy proponujemy dziesięcioprzedziałowy model COVID-19 z transmisją z człowieka na człowieka i ze środowiska na człowieka. Istotną cechą tego modelu jest uwzględnienie zarażonych, którzy uciekają z samoizolacji, a następnie rozprzestrzeniają chorobę. Model jest rygorystycznie analizowany zarówno teoretycznie, jak i numerycznie. Z matematycznego punktu widzenia udowadniamy, że stan wolny od choroby jest globalnie asymptotycznie stabilny, gdy  $\mathcal{R}_0^{av}$  jest mniejsze

niz jeden, czyli choroba wymiera. Gdy  $\mathcal{R}_0^{av}$  jest większe niż jeden, udowadniamy, że model dopuszcza unikalną równowagę endemiczną, lokalnie asymptotycznie stabilną, co oznacza, że choroba utrzyma się, przynajmniej wewnątrz basenu przyciągania równowagi endemicznej. Analiza wrażliwości modelu podkreśla, że transmisja środowiskowa jest najbardziej wpływowym parametrem, który prowadzi do rosnącej liczby zarażonych osobników, gdy tylko wzrasta. Nasz model został skalibrowany przy użyciu dziennych skumulowanych przypadków bezobjawowych w Rwandzie zgłoszonych od 1 kwietnia 2022 do 14 czerwca 2022. Stwierdziliśmy, że współczynnik odnowienia choroby jest równy 0,6479, a większość zarażonych osób w Rwandzie w tym okresie jest bezobjawowa. Badamy wpływ izolacji i samoizolacji w celu zmniejszenia obciążenia chorobą, a zarówno analiza wrażliwości, jak i analiza numeryczna pokazują, że izolacja ma większy wpływ na dynamikę infekcji niż samoizolacja.

*Klasyfikacja tematyczna AMS (2020):* 62J05; 92D20.

*Słowa kluczowe:* COVID-19; Izolacja; Samoizolacja; Transmisja środowiskowa; Uciekinier; Globalna stabilność; Analiza wrażliwości..



*Jean M.-S. Lubuma* is a Distinguished Professor at the University of the Witwatersrand, Johannesburg. He is doing research on Partial/ordinary differential equations; dynamical systems; numerical analysis (finite element/difference method, boundary element methods, etc.); function spaces (distributions, Sobolev, etc); integral equations of potential theory; mathematical biology/epidemiology; efficient numerical methods for nonlinear partial differential in fluid mechanics



*Arsène Jaures Ouemba Tassé* is currently a postdoctoral fellow at the University of the Witwatersrand at Johannesburg and a member of MaMoCLES research team at the University of Dschang. His field of research encompasses the Applied Dynamical Systems; Mathematical Modelling; Optimal control theory; Ordinary/partial differential equations; Manifolds theory; Bifurcation theory; Numerical analysis and Mathematical epidemiology. He obtained his PhD Degree in Applied Mathematics from the University of Dschang in Cameroon.




*Francis Signing* is a PhD student in applied mathematics at the University of Dschang, Cameroon. He has completed his PhD thesis examination process since June 2023 and is awaiting a formal public defense. His field of research is the applied dynamical systems with special interest in mathematical modeling of infectious diseases. He is a member of MaMoCLES research team at the University of Dschang.






of Dschang.


*Berge Tsanou* is a full professor of Applied Mathematics at the University of Dschang in Cameroon and an extraordinary professor at the University of Pretoria in South Africa. His research lies at the interface of dynamical systems, mathematical modeling and optimal control, with applications to population dynamics, human infectious diseases and crop diseases. He is the team leader of MaMoCLES, a research team on mathematical modeling and control in life and environmental sciences based at the University

JEAN M.-S. LUBUMA 


UNIVERSITY OF THE WITWATERSRAND JOHANNESBURG  
SCHOOL OF COMPUTER SCIENCE AND APPLIED MATHEMATICS  
UNIVERSITY OF THE WITWATERSRAND JOHANNESBURG, SOUTH AFRICA  
E-MAIL: [jean.lubuma@wits.ac.za](mailto:jean.lubuma@wits.ac.za)

ARSÈNE JAURES OUEMBA TASSÉ 

UNIVERSITY OF THE WITWATERSRAND JOHANNESBURG  
SCHOOL OF COMPUTER SCIENCE AND APPLIED MATHEMATICS  
UNIVERSITY OF THE WITWATERSRAND JOHANNESBURG, SOUTH AFRICA  
MONY KENG HIGHER INSTITUTE, BAFOUSSAM, CAMEROON  
E-MAIL: [arsene.ouembatasse@wits.ac.za](mailto:arsene.ouembatasse@wits.ac.za)

FRANCIS SIGNING 

UNIVERSITY OF DSCHANG  
DEPARTMENT OF MATHEMATICS AND COMPUTER SCIENCE  
DSCHANG, CAMEROON  
E-MAIL: [francis.signing@yahoo.fr](mailto:francis.signing@yahoo.fr)

BERGE TSANOU 

UNIVERSITY OF DSCHANG AND UNIVERSITY OF PRETORIA  
DEPARTMENT OF MATHEMATICS AND COMPUTER SCIENCE  
UNIVERSITY OF DSCHANG, CAMEROON  
DEPARTMENT OF MATHEMATICS AND APPLIED MATHEMATICS  
UNIVERSITY OF PRETORIA, SOUTH AFRICA  
E-MAIL: [bergetsanou@gmail.com](mailto:bergetsanou@gmail.com)

COMMUNICATED BY: Urszula Forys

(Received: 21st of March 2023; revised: 11th of January 2024)

---